Backreaction in an Analogue Black Hole Experiment

Sam Patrick,[1,*] Harry Goodhew,[2,†] Cisco Gooding,[1,‡] and Silke Weinfurtner[1,3,§]
[1]School of Mathematical Sciences, University of Nottingham, Nottingham NG7 2FD, United Kingdom
[2]Institute of Astronomy, University of Cambridge, Cambridge CB3 0HA, United Kingdom
[3]Centre for the Mathematics and Theoretical Physics of Quantum Non-Equilibrium Systems, University of Nottingham, Nottingham NG7 2FD, United Kingdom

(Received 4 July 2019; revised 14 December 2020; accepted 15 December 2020; published 29 January 2021)

Analogue models of gravity, particularly fluid mechanical analogues, have been very successful in mimicking the behavior of fields around black holes. However, hydrodynamic black holes are externally driven systems whose effective mass and angular momentum are set by experimental parameters, and, as such, no appreciable internal backreaction is expected to take place. On the contrary, we show using a rotating draining vortex flow that a fluid system of finite size responds to the presence of waves on timescales much longer than the wave dynamics, which leads to a significant global change in the total mass of our system. This backreaction is encapsulated by a dynamical metric, raising the possibility of studying backreaction in analogue black hole spacetimes.

DOI: 10.1103/PhysRevLett.126.041105

Introduction.—Analogue gravity, pioneered by Unruh in 1981 [1], is a research program that studies gravitational phenomena from general relativity (GR) using a wide variety of nongravitational systems (see Ref. [2] for a review). Unruh originally considered the propagation of sound waves through a fluid, and argued that if the fluid becomes supersonic in some region, the system exhibits a dumb hole horizon—the analogue of a black hole horizon. More generally, he showed that the wave equation describing the propagation of linear fluctuations ϕ through an ideal fluid is equivalent to the Klein-Gordon (KG) equation,

$$\frac{1}{\sqrt{-g}}\partial_\mu(\sqrt{-g}g^{\mu\nu}\partial_\nu\phi) = 0, \tag{1}$$

describing the propagation of a massless scalar field on an effective curved spacetime. The effective metric $g_{\mu\nu}$ describing such a spacetime is completely determined by the properties of the fluid flow under consideration, raising the intriguing possibility of studying general relativistic wave phenomena in the laboratory.

Many different analogues have since been investigated in a variety of condensed matter systems [3–8], including surface waves on top of a shallow fluid [9]. Although the analogy was originally conceived to investigate the trans-Planckian problem associated with Hawking radiation [10], analogue gravity has enjoyed a number of other successes: notably surface wave experiments have been used to measure Hawking radiation [11–13], superradiance [14], and quasinormal ringing [15].

One particularly simple model of a rotating black hole is provided by surface waves propagating on a rotating, draining fluid flow—the so-called draining bathtub vortex (DBT). Much work has been devoted to understanding features of this model (e.g., Refs. [16–26]), most of which relies on the assumption of an inviscid, incompressible, irrotational fluid in shallow water. Modifications resulting from the violation of these last two assumptions have been considered [27,28], and black hole effects (superradiance [14] and quasinormal ringing [15]) have been shown to persist under such conditions.

Another common assumption in many analogue gravity studies is that the waves propagate on a fixed background. This assumption is necessarily violated in both hydrodynamical and gravitational systems, since the fluctuations drive the evolution of the background through nonlinear terms in the equations of motion. This process in known as the backreaction. The usual justification for neglecting backreaction is that the nonlinear terms appear at quadratic order in perturbation theory and have little influence on the fluctuations, which are studied at linear order. However, since these terms can grow in time, they will eventually become important in determining the dynamics of the background. In atmospheric physics, this has widely been studied under the name wave-mean interaction theory [29] to predict large scale changes in atmospheric currents resulting from small perturbations. In studies of surface fluctuations, it has long been recognized that waves produce a second order mass flux in the direction of wave propagation [30], and that this mass flux induces a drift velocity called the Stokes drift [31,32]. Despite recognition from the fluid dynamics community, these effects have yet to be incorporated into the analogue gravity formalism.

In this Letter, we study the backreaction in an analogue black hole simulator by scattering surface waves with a DBT vortex. While the backreaction is to be expected in any

nonlinear system, it normally proceeds via a small local change in the background parameters. By contrast, we show that our system exhibits a significant global change in one of the background parameters: the total fluid mass. We demonstrate theoretically that this can be explained by way of the wave induced mass flux across the open boundary of a finite-sized system. Because of the analogy with black hole physics, this process induces a secular evolution in the effective metric, which occurs over much longer timescales than oscillations in the waves. Consequently, Eq. (1) holds over the full evolution and the description in terms of an analogue metric is applicable throughout. Hence, our system lends itself as a promising candidate for studying the backreaction due to superradiance and Hawking radiation.

Theory.—The system we are considering is a stationary draining fluid flow, where water enters a tank via an inlet and exits at a drain in a continuous cycle. Such a setup has previously been employed as a simulator for black hole superradiance [14] and ringdown [15] processes. For simplicity, we assume cylindrical symmetry about the drain and adopt polar coordinates (r, θ, z) centered on the drain. Water occupies a region $z \in [0, H]$ in the vertical direction. The area of the tank $\mathcal{A}$ (in the direction perpendicular to the vertical) is assumed constant and is bounded by the surface γ. For an incompressible fluid with density $\rho_f = \text{const}$, the system is fully characterized by the water height H and velocity field $\mathbf{V}$. Let γ be comprised of the surfaces $r = r_1$, encircling (and nearby) the drain, and $r = r_2$, which forms the outer wall of the tank. We assume the inlet condition is specified on a small section of $r = r_2$, but any θ dependence introduced is confined to a small layer at the edge of the tank which we neglect.

Now consider fluctuations (i.e., surface waves) described by $(h, \mathbf{v})$, which are switched on at $t = 0$ and are created inside $\mathcal{A}$. It is well known [30] that linear surface waves propagating on a background flow produce a mass flux $\mathbf{j}$ in the direction of wave propagation (which in our case is in the plane $\perp$ to the vertical). If the background $(H, \mathbf{V})$ is stationary for $t < 0$, then shortly after the onset of waves, the amount of mass M contained within the system will be altered if there is a net mass flux $\mathbf{j}_\perp = \rho_f \mathbf{v}_\perp$ over γ, according to

$$\dot{M} = -\int_\gamma \rho_f h \mathbf{v}_\perp \cdot d\mathbf{l}, \tag{2}$$

where the overdot denotes the time derivative and $d\mathbf{l} = \mathbf{r} d\theta$. The assumptions involved in the derivation of this formula are detailed in Appendix A of the Supplemental Material [33]. Furthermore, since $M = \rho_f \int_\mathcal{A} H dA$, a change in total mass results in a change in the water height. If we assume that H is approximately level over $\mathcal{A}$ (i.e., spatially uniform), then the water height adjusts according to

$$\dot{H}_0 \simeq -\frac{1}{\mathcal{A}} \int_\gamma h \mathbf{v}_\perp \cdot d\mathbf{l}, \tag{3}$$

where subscript 0 indicates that strictly a quantity is evaluated at $t = 0$. Expanding $H(t)$ around $t = 0$ gives

$$H(t) = H_0 + \dot{H}_0 t + \mathcal{O}(t^2). \tag{4}$$

The $\mathcal{O}(t^2)$ corrections become significant once changes to the background become large, which means that terms quadratic in the background variables also contribute to Eq. (3). Once this happens, the t dependence of H and $\mathbf{V}_\perp$ becomes interlinked and to solve the coupled system, one must use a second equation (the equation of momentum conservation) in addition to the equation of mass conservation which is used in the derivation of Eq. (2). Although we do not attempt this here, we expect this to produce exponential behavior of $H(t)$ at late times, since $\dot{H}$ will depend on the value of H.

Near $t = 0$, fluctuations of frequency ω perceive a quasi-stationary background and may be written,

$$f(t, \theta, r, z) = \sum_m f_m(r, z) e^{im\theta - i\omega t}, \tag{5}$$

where f is a placeholder for $(h, \mathbf{v})$ and we have also used our assumption of cylindrical symmetry to make a decomposition into modes of azimuthal number $m \in (-\infty, \infty)$. Using this ansatz, Eq. (3) becomes

$$\dot{H}_0 = -\frac{2\pi}{\mathcal{A}} \sum_m \frac{1}{2} \mathrm{Re}[h_m^* \mathbf{v}_m] \cdot \mathbf{r}|_{r_1}^{r_2}, \tag{6}$$

where $*$ denotes the complex conjugate and we have dropped the subscript $\perp$ on the velocity perturbation for conciseness. At $r = r_2$, $\mathbf{v}_m \cdot \mathbf{e}_r$ vanishes everywhere except at the inlet, where we assume a rapid influx of water (exceeding the propagation speed of the fluctuations) required to drive the high flow velocities. Therefore, since the fluctuations are generated inside $\mathcal{A}$, the total mass flux receives no contribution at $r = r_2$ and is determined solely by the form of the fluctuations at $r = r_1$. In Appendix B of the Supplemental Material [33], we show how Eq. (6) can be evaluated in the shallow water regime for a DBT vortex. This system exhibits an effective horizon at $r = r_h$ which we take as our inner boundary.

Experiments.—To test the prediction of a linear decrease of the water height, see Eqs. (4) and (6), and also to observe how long this behavior holds, we scatter monochromatic surface waves with a DBT vortex in a controlled experiment. The vortex is generated by pumping water at flow rate Q into a rectangular (2.65 m × 1.38 m) tank and allowing it to drain through a hole of radius $d = 2$ cm located in the center. Once the vortex is in equilibrium (determined by the constancy of Q and H_0) monochromatic surface waves are generated using a series of electrically controlled pistons. The change in water height $\Delta H = H - H_0$ is determined by illuminating the free surface with a laser

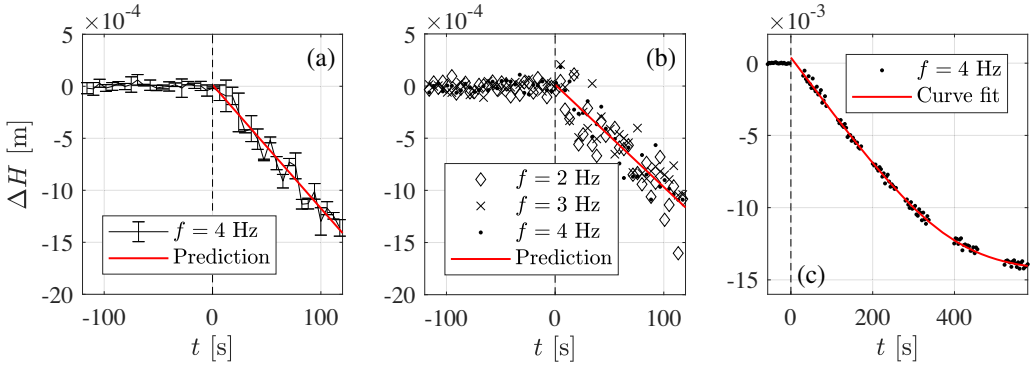

FIG. 1. The height change ΔH in a DBT resulting from wave incidence. The dashed vertical line indicates when the first wavefront passed the vortex. In experiment 1 (panel A), we find a consistent decrease in the water level when sending waves of frequency $f = 4$ Hz. We have plotted the average over three different repeats of the same experiment, and the error bars represent the standard deviation. In experiment 2 (panel B), we find similar behavior when sending waves of varying frequencies. The model is fitted to the average of the three datasets. In both experiments 1 and 2 we use the linear model in Eq. (4). In experiment 3 (panel C) we record the height change over a longer period of wave stimulation, finding good agreement with the heuristic fit in Eq. (7) which has exponential behavior at late times. Parameters obtained from the fits can be found in Table I.

sheet and tracking its average position with a high-speed camera. More details of the method can be found in Appendix C of the Supplemental Material [33].

In Table I of Ref. [33], we summarize the parameters used in each experiment. We display the measured $\Delta H(t)$ profiles in Fig. 1. In experiment 1 (panel A) we verify the linear decrease of H at early times predicted by Eq. (4). In experiment 2 (panel B) we test the frequency dependence of Eq. (6) by varying the frequency from 2 to 4 Hz, finding no significant variation of $\dot{H}_0$ within this range. In experiment 3 (panel C) we demonstrate that at late times the behavior of $H(t)$ deviates from a linear decline.

For the results of the first two experiments, we fit $\Delta H(t)$ with the linear decline predicted in Eq. (4) to provide a value for $\dot{H}_0$. Since we do not have a prediction for $H(t)$ over the full evolution, we devise a phenomenological model which has the expected behavior at early and late times, i.e., linear then exponential,

$$H(t) = H_0 + \frac{1}{2}\dot{H}_0(t+t_c) - \dot{H}_0\tau \log\left(2\cosh\left[\frac{t-t_c}{2\tau}\right]\right). \quad (7)$$

The extra parameters are the time t_c at which the evolution switches from linear to exponential, and the exponential decay time τ. Strictly speaking, this model has linear asymptotics in the limit $t \to -\infty$. However, the behavior at $t = 0$ is well approximated as linear provided $t_c > \tau$. The parameters obtained from the fits are also contained in Table I.

Discussion.—Across all experiments, we find linear behavior at early times, lending support to our prediction in Eq. (4). This behavior persists while $\Delta H \ll H_0$ as expected, which can be seen by comparing ΔH in Fig. 1 with the corresponding value of H_0 in Table I. The observed lack of frequency dependence in the second experiment is supported by computation of Eq. (6) assuming a shallow water flow (see Appendix B of the Supplemental Material [33]), which predicts that the value $\dot{H}_0$ only varies by $\sim 1\%$ over the range $f \in [2, 4]$ Hz. Furthermore, by comparing the gradients across the different experiments we see that $\dot{H}_0$ depends on H_0, supporting our claim that the late time behavior should be exponential. This is further evidenced by the late time tail in experiment 3.

In Fig. 2, we compare a simulation of the shallow water wave equation [see Eq. (B5) of the Supplemental Material [33]] for $H_0 = 2$ cm and $f = 2$ Hz with the scattered wave from experiment 2 for the same frequency. A mathematical justification of our inviscid, shallow water treatment for this particular experiment can be found in Appendix C of the Supplemental Material [33]. This treatment is corroborated by the clear similarities between experiment and simulation in Fig. 2. The scattered wave in our setup was measured using the air-water interface sensor described in Ref. [14] and for the simulation, we used the flow parameters $C = 0.013$ and $D = 0.001$ m^2/s with the velocity profile in Eq. (B2) of the Supplemental Material [33]. These values were chosen to be similar to that found from the flow measurements of Refs. [14,15], which involved the same experimental apparatus, and the precise values were tuned to match the number of wave fronts on the left and right sides of the images [44]. Using the form of the perturbations on the horizon, which requires knowledge of the transmission coefficient (see Appendix B of the Supplemental Material [33]), Eq. (3) predicts $\dot{H}_0 = -0.011$ mm/s. Comparing with the measured value $\dot{H}_0 = -9.8 \pm 0.2 \times 10^{-3}$ mm/s from in Table I, we find good agreement, despite the violation of $H \neq H(r)$ and $\nabla \times \mathbf{V} = 0$ (also assumed by our prediction) in the vortex core where the horizon is located (see Appendix C of the Supplemental Material [33] for further discussion).

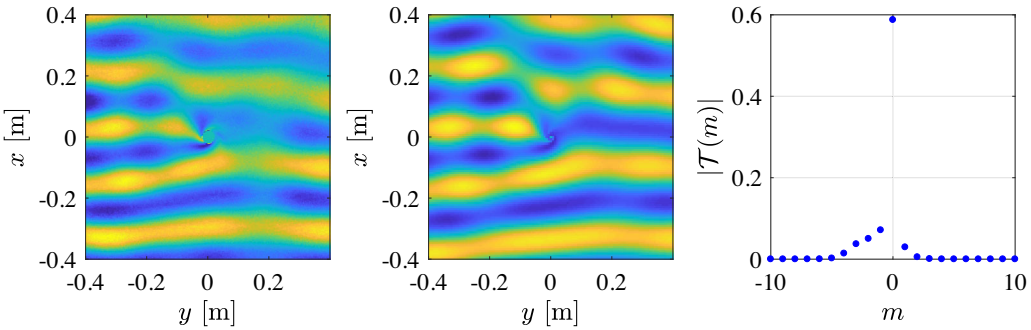

FIG. 2. Comparison between a scattered $f = 2$ Hz wave produced under the conditions of experiment 2 (left) and the prediction from a simulation of the shallow water equations for an irrotational vortex with a flat free surface (center). A plane wave is generated at $x < 0$ and propagates toward $x > 0$. The vortex rotates counterclockwise. On the left, the curvature of the free surface near the drain is too large for our detection method to resolve, and hence we exclude data points for $r < d$. The similarity between the two images is apparent, thereby supporting our simplified theoretical treatment. We also display the transmission coefficients $\mathcal{T}_m$ (right) obtained from the simulation, which enter into the equation for $\dot{H}_0$ via the transmitted wave amplitude $|A^h_m| = \mathcal{T}_m(ga/\omega)(2\pi\omega/c)^{-1/2}$ [see Eq. (B8) in the Supplemental Material [33]]. Therefore, only the low lying m modes (and mainly those with $m \leq 0$) contribute to ΔH.

To relate the effect we have observed to the backreaction in GR, consider the following. For slowly evolving background, one can adopt different timescales for the background and the fluctuations (i.e., a Born-Oppenheimer approximation [45]). In this approximation, which is also employed to study the backreaction in GR [46], the fluctuations of a shallow water, irrotational fluid obey Eq. (1), with the components of the evolving effective metric given by

$$g_{\mu\nu} = \begin{pmatrix} -(gH - V_{\perp,i}V^i_\perp) & -V_{\perp,i} \\ -V_{\perp,j} & \delta_{ij} \end{pmatrix}, \tag{8}$$

where the indices i and j run over spatial dimensions, δ_{ij} is the Kronecker delta function and the t dependence enters via $H(t)$ and $\mathbf{V}_\perp(t) = V^i_\perp(t)\mathbf{e}_i$. In our analysis, we have estimated only $H(t)$ a short time after the beginning of wave incidence and the full dynamics of $H(t)$ and $\mathbf{V}_\perp(t)$ warrant further investigation. Furthermore, since the energy and angular momentum density of the shallow water background flow are given by $\mathcal{E} = \frac{1}{2}H\mathbf{V}^2_\perp$ and $L = H\mathbf{r} \times \mathbf{V}_\perp$, respectively, a change in H corresponds to changes in both $\mathcal{E}$ and L. Therefore, the height change mediates the exchange of energy and angular momentum between the waves and background.

Although the analogy persists at the linear level, the backreaction equation, describing how the effective metric evolves, is specific to the equations of motion of the system under consideration, which are the Euler equations for ideal fluids and the Einstein equations in GR (different backreaction equations have been studied, for example, in Refs. [46–49]). Despite this, it may still be possible to learn about generic features of slowly backreacting spacetime geometries using analogue systems. In addition, it is possible extract scattering amplitudes from changes in global parameters (here the water height) for controlled scattering processes, e.g., scattering of waves with a single azimuthal wave number.

Conclusion.—In this work, we have studied the backreaction of surface waves on a draining vortex flow. Our results demonstrate that surface waves interacting with an initially stationary vortex will trigger the evolution of the background out of equilibrium. Because of the flow being externally driven, it was previously unclear whether the background had the freedom to adjust to the presence of waves in analogue gravity simulators. Our findings show that the backreaction is indeed observable, and that the system does in fact have freedom to redistribute energy and angular momentum between the incident waves and the background flow. In the shallow water regime, we have argued that this evolution is encapsulated by a dynamical effective metric. Although this metric does not evolve according to the Einstein equation, further similarities between slowly evolving gravitational and analogue spacetimes have yet to be investigated.

This realization is important for a number of reasons. First, one must ensure that any wave effects (e.g., stimulated Hawking radiation, superradiance, and quasinormal ringing) are measured on a timescale much shorter than the time it takes for the background to change, so that the assumption of a stationary background is not violated. This may restrict the frequency range one can probe in an analogue gravity experiment, as nonlinear effects will influence the low frequency behavior which takes places over longer timescales. Second, the effect we have described is a global (as opposed to local) phenomenon. Thus, one can use the asymptotic value of the water height to obtain insight into scattering processes, similar to the role that the black hole mass plays in GR.

Based on previous experience, a similar behavior is expected to occur in suitable quantum systems, and thus our findings suggest that analogue gravity experiments can be used to cross validate backreaction models in a relativistic setting. This is an area of research where lack of experimental input is stalling theoretical development.

S. W. acknowledges financial support provided under the Paper Enhancement Grant at the University of Nottingham, the Royal Society University Research Fellow (UF120112), the Nottingham Advanced Research Fellow (A2RHS2), the Royal Society Enhancement Grant (RGF/EA/180286) and the EPSRC Project Grant (EP/P00637X/1). S. W. acknowledges partial support from STFC consolidated Grant No. ST/P000703/. We also want to thank T. Torres, S. Erne, Z. Fifer, A. Geelmuyden, and T. Sotiriou for many useful discussions, as well as J. Louko, W. G. Unruh, and R. M. Wald for their insightful feedback.

*sampatrick31@googlemail.com
†hfg23@cam.ac.uk
‡cisco.gooding@nottingham.ac.uk
§silkiest@gmail.com

[1] W. G. Unruh, Phys. Rev. Lett. **46**, 1351 (1981).
[2] C. Barcelo, S. Liberati, and M. Visser, Living Rev. Relativity **14**, 3 (2011).
[3] G. Rousseaux, C. Mathis, P. Maïssa, T. G. Philbin, and U. Leonhardt, New J. Phys. **10**, 053015 (2008).
[4] J. Steinhauer, Nat. Phys. **10**, 864 (2014).
[5] J. Steinhauer, Nat. Phys. **12**, 959 (2016).
[6] F. Belgiorno, S. L. Cacciatori, M. Clerici, V. Gorini, G. Ortenzi, L. Rizzi, E. Rubino, V. G. Sala, and D. Faccio, Phys. Rev. Lett. **105**, 203901 (2010).
[7] D. Vocke, C. Maitland, A. Prain, K. E. Wilson, F. Biancalana, E. M. Wright, F. Marino, and D. Faccio, Optica **5**, 1099 (2018).
[8] Z. Fifer, T. Torres, S. Erne, A. Avgoustidis, R. J. A. Hill, and S. Weinfurtner, Phys. Rev. E **99**, 031101(R) (2019).
[9] R. Schützhold and W. G. Unruh, Phys. Rev. D **66**, 044019 (2002).
[10] W. G. Unruh and R. Schützhold, Phys. Rev. D **71**, 024028 (2005).
[11] L. P. Euvé, F. Michel, R. Parentani, T. G. Philbin, and G. Rousseaux, Phys. Rev. Lett. **117**, 121301 (2016).
[12] S. Weinfurtner, E. W. Tedford, M. C. J. Penrice, W. G. Unruh, and G. A. Lawrence, Phys. Rev. Lett. **106**, 021302 (2011).
[13] S. Weinfurtner, E. W. Tedford, M. C. J. Penrice, W. G. Unruh, and G. A. Lawrence, in *Analogue Gravity Phenomenology* (Springer, New York, 2013), pp. 167–180.
[14] T. Torres, S. Patrick, A. Coutant, M. Richartz, E. W. Tedford, and S. Weinfurtner, Nat. Phys. **13**, 833 (2017).
[15] T. Torres, S. Patrick, M. Richartz, and S. Weinfurtner, Phys. Rev. Lett. **125**, 011301 (2020).
[16] S. Basak and P. Majumdar, Classical Quantum Gravity **20**, 3907 (2003).
[17] S. Basak and P. Majumdar, Classical Quantum Gravity **20**, 2929 (2003).
[18] V. Cardoso, J. P. S. Lemos, and S. Yoshida, Phys. Rev. D **70**, 124032 (2004).
[19] E. Berti, V. Cardoso, and J. P. S. Lemos, Phys. Rev. D **70**, 124006 (2004).
[20] M. A. Anacleto, F. A. Brito, and E. Passos, Phys. Lett. B **703**, 609 (2011).
[21] S. R. Dolan, L. A. Oliveira, and L. C. B. Crispino, Phys. Rev. D **85**, 044031 (2012).
[22] S. R. Dolan and E. S. Oliveira, Phys. Rev. D **87**, 124038 (2013).
[23] M. Richartz, A. Prain, S. Liberati, and S. Weinfurtner, Phys. Rev. D **91**, 124018 (2015).
[24] D. Dempsey and S. R. Dolan, Int. J. Mod. Phys. D **25**, 1641004 (2016).
[25] S. Churilov and Y. Stepanyants, Phys. Rev. Fluids **4**, 034704 (2019).
[26] A. Banerjee, R. Koley, and P. Majumdar, arXiv:1808.01828.
[27] S. Patrick, A. Coutant, M. Richartz, and S. Weinfurtner, Phys. Rev. Lett. **121**, 061101 (2018).
[28] T. Torres, A. Coutant, S. R. Dolan, and S. Weinfurtner, J. Fluid Mech. **857**, 291 (2018).
[29] O. Bühler, *Waves and Mean Flows* (Cambridge University Press, Cambridge, England, 2014).
[30] O. M. Phillips, *The Dynamics of the Upper Ocean* (Cambridge University Press, New York, 1966).
[31] K. E. Kenyon, J. Geophys. Res. **74**, 6991 (1969).
[32] K. Hasselmann, J. Fluid Mech. **15**, 273 (1963).
[33] See Supplemental Material at http://link.aps.org/supplemental/10.1103/PhysRevLett.126.041105, for more details on the derivation of the height change formula (A), the height change in a shallow water draining vortex (B), our experimental procedure (C) and a discussion of conserved currents in the system (D), which includes Refs. [19,23,25,30,34–43].
[34] L. D. Landau and E. M. Lifshitz, *Fluid Mechanics* (Elsevier, New York, 1987).
[35] M. Visser, Classical Quantum Gravity **15**, 1767 (1998).
[36] O. Ganguly, arXiv:1705.04935.
[37] W. G. Unruh, in *Analogue Gravity Phenomenology* (Springer, New York, 2013), pp. 63–80.
[38] A. Coutant and R. Parentani, Phys. Fluids **26**, 044106 (2014).
[39] S. E. P. Bergliaffa, K. Hibberd, M. Stone, and M. Visser, Physica (Amsterdam) **191D**, 121 (2004).
[40] S. Liberati, S. Schuster, G. Tricella, and M. Visser, Phys. Rev. D **99**, 044025 (2019).
[41] M. Srednicki, *Quantum Field Theory* (Cambridge University Press, Cambridge, England, 2007).
[42] M. D. Schwartz, *Quantum Field Theory and the Standard Model* (Cambridge University Press, Cambridge, England, 2014).
[43] P. Meystre and M. Sargent, in *Elements of Quantum Optics* (Springer, New York, 2007), pp. 1–34.
[44] Changing the values of C and D by 10% resulted in notable visual discrepancies between the two scattering patterns in

Fig. 2. The predicted value of $\dot{H}_0$ changed by about 60% when using these values.

[45] M. Born and R. Oppenheimer, Ann. Phys. (Berlin) **389**, 457 (1927).

[46] R. Balbinot, A. Fabbri, S. Fagnocchi, and R. Parentani, Riv. Nuovo Cimento **28**, 1 (2005).

[47] R. Balbinot, S. Fagnocchi, and A. Fabbri, Phys. Rev. D **71**, 064019 (2005).

[48] R. Schützhold, M. Uhlmann, Y. Xu, and U. R. Fischer, Phys. Rev. D **72**, 105005 (2005).

[49] R. Schützhold, Proc. Sci. QG-PH2007 (**2007**) 036 [arXiv:0712.1429].